

# Stable and Flexible Multi-Vehicle Navigation Based on Dynamic Inter-Target Distance Matrix

José Vilca<sup>id</sup>, Lounis Adouane, and Youcef Mezouar

**Abstract**—This paper proposes a flexible multi-layer and multi-controller architecture for a dynamic navigation in the formation of a group of autonomous vehicles in constrained environments. The main objectives of this architecture are to ensure reliable navigation in the formation of the vehicles and to guarantee the stable and smooth reconfiguration of the fleet shape. A precise review and analysis of the main used *leader-follower* modeling for the control of a fleet of autonomous vehicles is conducted. After highlighting their advantages and drawbacks, an appropriate *leader-follower* approach based on deformable shape is proposed. At each sample time, the leader's state (pose and velocity), defined as the main dynamic target, is taken as a reference to guide the overall fleet dynamic. In addition, an analytic formulation of the maximum linear and angular velocities of the leader is proposed in order to guarantee the asymptotic stability of the navigation in formation as well as the fleet reconfiguration phases (between different formation shapes). An important focus of this paper corresponds to the proposition of a reliable strategy for the fleet reconfiguration, according to the environmental context (when, for instance, obstacles are detected). The safety of the fleet is formally demonstrated using an appropriate reconfiguration matrix, which takes into account the vehicles' set-points inter-distances to avoid any inter-vehicles collisions. In addition, an estimation of the formation parameters, according to an authorized minimum distance between the vehicles, is given. Simulations and experiments in different scenarios are performed to demonstrate the flexibility, reliability, and efficiency of the proposed dynamic navigation of a fleet of vehicles in formation.

**Index Terms**—Cooperative autonomous vehicles, navigation in formation, dynamic reconfiguration, modular control architecture, inter-target distance matrix.

## I. INTRODUCTION

THE Navigation in Formation (NiF) of multiple autonomous vehicles in dynamic environments constitutes one of the fundamental issues for systems of Multi-Unmanned Ground Vehicles (MUGVs) [1], [2]. Indeed, an important part of the tasks performed by MUGVs

Manuscript received August 5, 2017; revised January 20, 2018, April 9, 2018, and June 6, 2018; accepted June 16, 2018. This work was supported by the Agence Nationale de la Recherche (ANR) and the Agence de l'Environnement et de la Maîtrise de l'Energie (ADEME) through the SafePlatoon project, research programs Investissements d'Avenir of RobotEx Equipment of Excellence under Grant ANR-10-EQPX-44 and the IMoBS3 Laboratory of Excellence under Grant ANR-10-LABX-16-01. The Associate Editor for this paper was S. Kong. (Corresponding authors: José Vilca; Lounis Adouane.)

The authors are with the Institut Pascal, Université Clermont Auvergne/SIGMA-UMR CNRS 6602, 63000 Clermont-Ferrand, France (e-mail: FirstName.LastName@uca.fr).

Color versions of one or more of the figures in this paper are available online at <http://ieeexplore.ieee.org>.

Digital Object Identifier 10.1109/TITS.2018.2853668



Fig. 1. Autonomous navigation in formation of a group of UGVs in an urban environment (Clermont-Ferrand, France).

requires reliable and online control of the UGVs' mutual locations during the navigation. Among the main domains which draw a big interest for this kind of cooperative navigation, let us cite: public transportation in different areas (e.g., urban or/and highway) [3], [4], goods transportation in warehouses [5], agriculture [6] or military mission [7]. The NiF task raises several important scientific issues, such as: Control architectures for MUGVs; MUGVs planning and re-planning; MUGVs tracking; Cooperative perception and localization; MUGVs task allocation and communication [1], [2], [4], [8]–[11]. It is to be noticed that the driverless car is not only synonym of a car as we commonly known, but with the automation of its displacement functions. Indeed, in parallel with the developments of this area by automotive industries, another generation of UGVs like VIPALAB (cf. Fig. 1) aims also to autonomously transport passengers but in a more restricted area like midtown or inside big companies, amusement parks, airports, etc. which need autonomous shuttles between their different areas. Although the environment of navigation is generally delimited and the dynamic of the UGVs is not the same as for the Google car [12] for instance, nevertheless an important part of the autonomous navigation issues are shared. Indeed, this kind of UGVs must, like the Google car, navigate autonomously while taking into account the different events (e.g., obstructing objects, vehicles' coordination, intersection crossing, etc.). The proposed paper makes the focus on dynamic NiF for passengers' transportation in urban environments based on an appropriate MUGVs control architecture (cf. Section III) and a dedicated strategy of planning and re-planning of the MUGVs formation configuration and reconfiguration (cf. Sections IV and V).

This last decade, several ambitious projects, such as SARTRE (Safe Road TRains for the Environment, [13]) or GCDC (Grand Cooperative Driving Challenge [14]), have involved a fleet of UGVs, navigating in formation. The platoon<sup>1</sup> navigation for passengers' transportation is among the most investigated MUGVs' formation pattern [2], [15], [16]. It is motivated mainly in order: *i*) to reduce the UGVs' energy consumption, while enhancing the overall fleet aerodynamics (minimize air drag, such as cyclists in platoon); *ii*) to provide promising solutions to traffic congestion (reduce/condensate the occupancy space), since UGVs can be much closer to each other; *iii*) to have safer and more comfortable driving with the help of better coordination between the UGVs [17], [18]. Even if the platooning pattern is among the most common shape for the NiF, nevertheless other formation patterns are also important to achieve specific tasks. It is clearly stated for agriculture [6] or military [7] applications for instance, but it is also important for passengers' transportation, to deal with more complex situations, necessitating much more fleet coordination and reconfiguration. Indeed, it is the case for instance for a fleet of UGVs which has to perform merging and/or splitting maneuvers in order to enter or to go out (disengage) in a highway or another road. These merging/splitting maneuvers, which could involve either only one UGV [19] or a multitude of them at a time [20], can be seen as a formation reconfiguration with a transitional phase to master. Thus, having a control architecture which shows a high flexibility and safety features, to deal with several formation configuration and reconfiguration, is an important issue. This paper deals with stable and flexible passengers' transportation using a fleet of urban vehicles (cf. Figure 1), performing generic dynamic shape configuration and reconfiguration. The platooning formation is thus only one among the possible examples of formation shapes which can be ensured by the overall proposed control architecture and its different mechanisms (cf. Sections III to V).

In the following section II, the motivation and related work are discussed.

## II. MOTIVATION AND RELATED WORKS

To have a clear view of the proposed overall control architecture to manage the MUGVs. Subsection II-A discusses the main concepts highlighted in the literature in order to lead toward the proposed Multi-Layer and Multi-Controller (MLMC) architecture (which is afterward detailed in Section III). In Subsection II-B, the focus is made more on the motivation and the related works dealing with dynamic navigation in formation of a fleet of UGVs.

### A. Control Architectures for MUGVs

One of the key issues to fix before the development of MUGV control architecture, corresponds to the possibility to centralize the control or to decentralize (distribute) it on the

robotics entities [21]. An architecture is called centralized, when a part or all of the sensory and/or decisional loops of each robotic entity is unlocalized w.r.t. its physical structure, and managed by a central unit, called supervisor [22]. A centralized architecture implies a global knowledge of each element of the system and requires high computational power, massive information flow and generally not robust, due to the dependence on a single controller/supervisor. In contrast, in a decentralized control approach, each UGV of the system has its own perceptions/decisional process. This kind of control implies a reduced number of communicated signals and data knowledge. In fact, each robotic entity does not need to have the overall environment knowledge before acting on its environment. Decentralized control, if well mastered, is then more flexible to deal with MUGVs having a large number of entities. The possibility also exists to centralize only a part of the control and let the other part be decentralized (hybrid (centralized/decentralized) control) [23]. The centralized control is applied to determine the general strategies and tasks to be performed by the MUGVs, and the decentralized part takes over for the navigation and local actions. Besides of the centralized/decentralized aspect for controlling a MUGVs systems, a consensus is usually adopted in the literature on the structure of the architecture, which exhibiting at the same time cognitive (or deliberative) and reactive features [24]. These architectures are generally structured in three layers [25]: the highest level is responsible for mission planning and re-planning; the intermediate layer activates the low-level behaviors and permits passing of parameters to them; while the lowest level layer contains the physical sensor and actuators' interfaces. The cognitive part (highest level) contains generally a symbolic world model (based on artificial intelligence concepts), which develops plans and makes decisions on the way to perform the UGVs' objectives. The reactive part (the two other lower levels) are responsible for reacting to local events without complex reasoning. Nevertheless, generally the structural conception of these hybrid architectures remains too complex to manage the different levels of hierarchy imposed by this kind of architectures. They are also low harmonized to deal with the effective set-points to send to the robot actuators (lowest level). Efforts have been more concentrated on the conceptual aspects (using for instance the multi-agent paradigm to manage the multi-layered proposed architectures [26]) and less on the overall architecture simplicity, generality and its effective implementation on the UGVs. Indeed, even if the control architecture must show a good level of knowledge abstraction and decision, it is important to translate them in terms of low-level robot control set-points to exhibit clearly its effects on the robots' movements, which permit at its turns to attest on the safety and on the overall control architecture stability [27].

It is proposed in section III an overall MLMC architecture for dynamic NiF. This architecture exhibits hybrid (centralized/decentralized as well as cognitive/reactive) features and is designed to be enough generic to be used with only one control law for any controller, composing the overall architecture. This imposes also to use generic set-points definition based on static/dynamic targets (cf. Section IV).

<sup>1</sup>Where each UGV has as objective to follow another one while maintaining a determined longitudinal constant distance (either Euclidean or curvilinear (cf. Section V-A)) to the vehicle ahead.

### B. Dynamic Navigation in Formation of a Fleet of UGVs

The control of a group of UGVs navigating in formation is addressed in the literature while mainly adopting three strategies: *i) behavior-based* [28] (called also multi-controller architecture [1]); *ii) virtual structure* [29]; and *iii) leader-follower* [30]. The behavior-based formation control relies on coupled dynamics (relative position and velocity) between neighbor robots [31]. A static and dynamic virtual structure based on Lyapunov approach was proposed in [32]. A virtual structure with obstacle avoidance for a group of Unmanned Aerial Vehicles (UAV) was proposed in [33]. The approach uses a penalty function (distance to the virtual target and/or obstacle) and a priority strategy (according to the distance w.r.t. other UAVs or obstacles). The control law uses the Model Predictive Control (MPC) based on time horizon and optimization of a specific cost function. A cooperative co-evolutionary algorithm-based on MPC is also proposed in [34] with a guarantee to achieve the MUGVs formation. Even if the use of MPC gives a very interesting results, nevertheless, this method is generally time consuming, due mainly to the predictive computation and constrained optimization w.r.t. the time horizon. These approaches are very flexible and extensible to more complex tasks, nevertheless, it is difficult to guaranty the stability of the overall system during the transition between the different behaviors and/or tasks which can lead to non-defined behaviors and/or to commands outside the limits. Furthermore, these approaches do not address issues related to the constraints of the formation shape and to the vehicle's kinematics.

The case of dynamic formation reconfiguration (DFR) has been dealt with several other works such as in [35], [36], or [37]. In [35], switches between different formation shapes are exploited (from triangle to line) to avoid encountered obstacles in the environment. The formation control law is based on input-output feedback linearization and vision sensors (omnidirectional camera) are embedded in each robot for localization and navigation purpose. A decentralized gradient control law to stabilize a group of point mass robots to any formation corresponding to an infinitesimally rigid framework was proposed in [38]. In [36], the leader UGV generates a free-collision trajectory in a dynamic environment which is tracked using a formation control law based on neural network, Lyapunov function and UGV's dynamical model. The stability of the dynamic formation and dynamic topology (adjacency matrix) are also demonstrated. A strategy to reshape the formation configuration by scaling the distance between the vehicles is proposed in [37]. In this last reference, obstacle avoidance for the group of UGVs is addressed using potential fields. A non-rigid formation control, where the most appropriate UGVs' positions (formation shape) are determined according to a directional visual perception is proposed in [39]. The inter-robot communication allows choosing the leader of the group. Several works in the literature focus on the definition of the negotiation protocol between UGVs to define their role in the fleet [40], [41]. In [40] each vehicle is assigned a specific role in the maneuver, and this eases the definition of the protocol. Instead, the authors in [41] define a protocol to

coordinate the information exchange within UGVs to perform merging maneuvers between two platoons.

In addition to the proposition of an overall MLMC architecture (cf. Section III), this paper proposes a new Strategy for Formation Reconfiguration (SFR) based on *leader-follower* and behavioral approach. The *leader-follower* approach (cf. Section IV) allows to the central entity (the leader) to manage safely and smoothly the configuration and reconfiguration of the formation shape (cf. Section V). The behavior-based approach allows to each UGV (follower) to reliably track its assigned virtual target while avoiding, if necessary, any detected obstacle. This paper is organized as follows, next section presents the proposed control architecture of the MUGVs system. The proposed navigation in formation based on *leader-follower* and *behavior-based* approaches according to the leader's reference frame is described in Section IV. Section V presents the proposed reconfiguration methods for the MUGVs dynamic formation. An analysis of the formation constraints (geometric and kinematics), stability and parameter design is also detailed in this section. Simulations and experiments are given in sections V and VI to show the reliability of the different proposals. Finally, this paper ends with a conclusion and some prospects in Section VII.

### III. CONTROL ARCHITECTURE FOR MULTI-VEHICLE NAVIGATION

This section makes the focus on the structure and the main blocks composing the overall proposed MLMC architecture in order to ensure flexible, smooth and safe dynamic NiF of the MUGVs system. This architecture is composed of several layers (the brief details of each layer are given in Subsections III-A to III-D) in order to reliably control both: the autonomous navigation of each UGV in cluttered environments and the hybrid (centralized/decentralized) coordination of the fleet of UGVs in formation (cf. Section II-A). The centralized part corresponds to the use of *leader-follower* approach, where the leader plays the role of a central entity inducing the overall fleet set-points dynamic (cf. Section IV) and the decentralized (or distributed) aspect corresponds to the fact that when the formation set-points are already defined, then each follower UGV will follow in a fully distributed way its assigned set-point in order to maintain the formation shape or to reconfigure it (cf. Section V). It is important to mention that each UGV composing the fleet of vehicles has the same homogeneous MLMC architecture. Thus, the leader as much as the followers are embedded with this same architecture, hence, it is straightforward to switch the role between the leader ( $UGV_L$ ) and one of the followers ( $UGV_F$ ) according to the task to achieve or to the navigation context. The *Executive* layer (cf. Fig. 2 and subsection III-C) is responsible to define the UGVs roles. Furthermore, unlike what has been developed in [42], [43], or [44], where the assignment of the leader or the choice of the position of each follower in the formation is obtained dynamically (according to the navigation context), it is considered in what follows that the role of both: the leader and the followers are assigned once and for all, during each of the simulations / experiments shown in Sections V and VI.

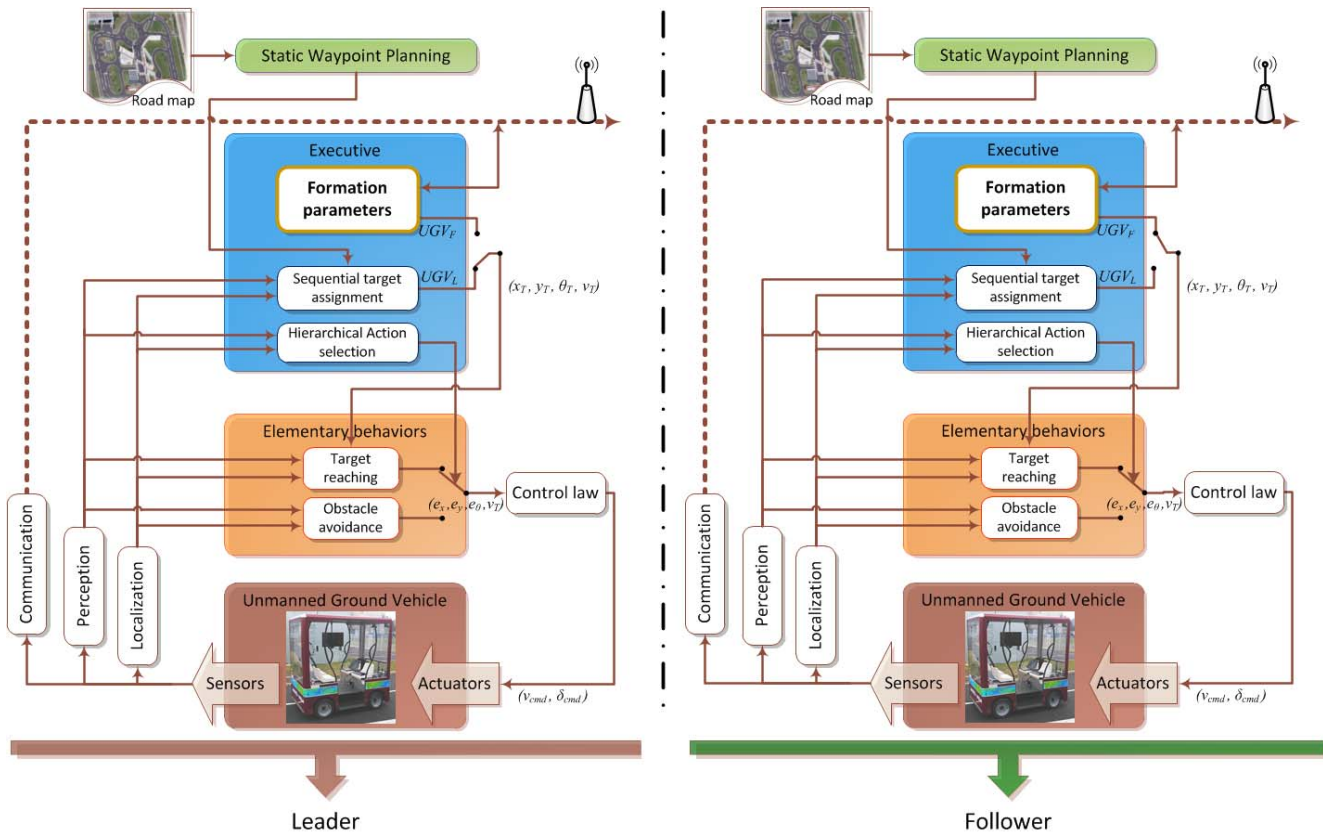


Fig. 2. Multi-Layer and Multi-Controller (MLMC) architecture, embedded in each UGV, for the navigation in formation of the fleet.

This choice has been made also to make the focus in this paper only on the main proposals related to the dynamic navigation and reconfiguration of the MUGV system.

The proposed MLMC aims also to manage the interactions among elementary behaviors while guaranteeing the stability of the overall control [45]. It allows obtaining safe and smooth navigation of UGVs (cf. Section VI). The used UGVs are modeled as tricycle mobile robots (cf. Subsection III-A) and an appropriate control law, based on Lyapunov synthesis, has been used to control the UGV movements [46] (cf. Subsection III-B). In addition to the proposed overall MLMC architecture, this paper mainly focuses on the development of an appropriate strategy of navigation in formation and its safe and dynamic reconfiguration, according to the navigation context. These latter aspects are described and analyzed in detail in Sections IV and V respectively. Nevertheless, for the clarity of this paper, some details about each layer / controller are summarily given below and in the following subsections.

The *Localization* block uses sensor information to estimate the current pose of UGV [47]–[49]. In this work, an RTK-GPS and an IMU (Inertial Measurement Unit) embedded in each vehicle are combined using Extended Kalman Filter (EKF) to allow accurate estimation of the current configuration (cf. Section VI).

The *Perception* block captures information related to the UGV’s environment as potential obstacles via range sensors or cameras [50]–[52]. In this work, the UGV’s perception uses data from a range sensor LIDAR. The observed data

allows to identify online obstacles and surround them with the closest ellipse used as input of an obstacle avoidance approach based on elliptical limit-cycle [53], [54].

The *Communication* block is related to the UGV’s capability to send and to receive information from other UGVs. In this work, the UGV’s information (e.g., current pose and velocity) uses UDP protocol for message transmission and reception. Each UGV has Wi-Fi wireless antennas for communication.

Before describing shortly each layer of the control architecture (cf. Fig. 2), let us present the used model for the vehicle.

#### A. Modeling of Vehicle: Kinematic Model

We assume UGV evolves in asphalt road and in cluttered urban environment with relatively low speed (less than 3 m/s). Hence, the use of kinematic model (which relies on pure rolling without slipping) of UGV is sufficient. The kinematic model is based on the well-known tricycle model [55]. The two front wheels are replaced by a single virtual wheel located at the center between the front wheels. The equations of UGV’s model can be written as (cf. Fig. 3):

$$\begin{cases} \dot{x} = v \cos(\theta) \\ \dot{y} = v \sin(\theta) \\ \dot{\theta} = v \tan(\gamma) / l_b \end{cases} \quad (1)$$

where  $(x, y, \theta)$  is the UGV’s pose in Global reference frame  $X_G Y_G$ .  $v$  and  $\gamma$  are respectively the linear vehicle’s velocity

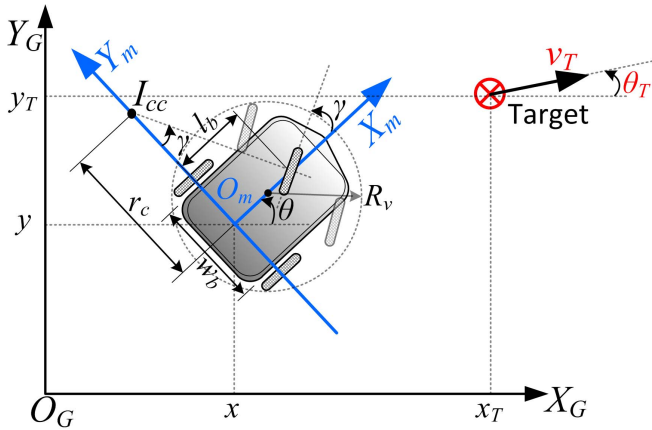


Fig. 3. Vehicle's configuration in Global ( $X_G Y_G$ ) and Local ( $X_m Y_m$ ) reference frames.

and the orientation of the vehicle's front wheel.  $l_b$  is the vehicle's wheelbase.  $I_{cc}$  is the instantaneous center of curvature of the vehicle's trajectory,  $r_c = l_b / \tan(\gamma)$  is the radius of curvature and  $c_c = 1/r_c$  is the curvature.

### B. Elementary Behaviors Layer

This layer contains different elementary motion controllers to perform sequentially several sub-tasks (cf. Fig. 2). The UGV's navigation is operated by two elementary controllers (behaviors): (*Target reaching* and *Obstacle avoidance*). At each sample time one of them is activated by *Decision making* block (executive layer (cf. Subsection III-C)) according to the perceived environment (*Perception* block). Each elementary controller provides as output an error state (depending on the pose and velocity of the vehicle w.r.t. the defined set-points (cf. Section IV) to the *Control law* block which permits us to guarantee asymptotic stability of the control law [56]. Thus, the used multi-control architecture has been designed to use a single control law for the different elementary behaviors. This control law allows the UGV to reach either static or dynamic targets (more details are given in [46] and [56]).

### C. Executive Layer

This layer contains the *Decision making* block to manage the elements of the behavioral layer (*Hierarchical action selection*) [57] and the selection of next waypoint to be reached by the UGV (*Sequential target assignment*) [46]. The *Hierarchical action selection* is dedicated to manage the switches between *Target reaching* and *Obstacle avoidance* behaviors, according to the environmental perception. The *Hierarchical action selection* activates the *Obstacle avoidance* block as soon as it detects at least one obstacle which can hinder the future vehicle movement toward its assigned target (more details are given in [54] and [58]). This action allows to anticipate the activation of obstacle avoidance behavior and to decrease the time to reach the assigned target (especially in very cluttered environments) instead of activating the obstacle

avoidance only when the robot is in the immediate vicinity of the obstacle [58].

The *Sequential target assignment* allows to an UGV, when it becomes the leader, to perform autonomous navigation through successive static waypoints, suitably disposed in the environment [46]. These waypoints are obtained by a method which selects the optimal set of waypoints [59] to perform safe vehicle navigation in cluttered environment (cf. Subsection III-D). To navigate between successive waypoints, the distance and orientation errors between the vehicle and current assigned waypoints are considered. An error threshold is used to switch to the next waypoint in the sequence. The value of the threshold is related to the inaccuracies of the vehicle localization and/or the performance of the used control law [46]. The waypoint set-point is updated with the next waypoint (already pre-sorted in an appropriate list [59]), which should not intersect with any obstacle (otherwise, a new next waypoint is selected until this condition is satisfied). Finally, the vehicle switch to reach this new waypoint and so on.

The *Formation parameters* block is designed to generate several virtual dynamic targets  $T_{d_i}$  that each UGV follower  $i$  has to track using the proposed target-reaching control [46] (cf. Subsection III-B). The dynamics of the followers' set-points depend on the leader dynamic (*leader-follower* approach). This strategy allows a good flexibility and reliability of the formation shape modeling and control (cf. Section IV).

### D. Planning Layer

This layer encloses *Static Waypoint Planning*. This latter contains an efficient and flexible algorithm to obtain an optimal set of waypoints configuration in the environment [59]. The method is based on multi-criteria optimization and expanding tree to obtain the optimal waypoints configuration in cluttered environment. The optimization methodology takes into account the kinematic constraints of the vehicles (non-holonomy, maximum velocity and steering angle) and localization uncertainties, in order to obtain safe and efficient navigation of vehicles through sequential waypoints. It is to be noted that the configuration of the waypoints in the environment can take into account the desired shape of the multi-vehicle formation, for instance, in order to always avoid the road borders [59]. It is important to highlight that the waypoints planning could be done either offline or online, according whether the environment is static or not and that the overall planning process could be performed in real-time or not [59]. Hence, according of the kind of short or long-term planning, characterizing this planning layer, the overall MLMC can shows either reactive or cognitive features [24].

In this paper and as mentioned in subsection III-C, since the surrounding environment is considered enough static, only an optimal set of waypoints is used by the leader (as static set-points), in order to navigate safely and smoothly between them [46]. Concerning the followers' set-points, which depend on the leader dynamic (cf. Section IV), the followers' kinematic constraints and the desired shape to reach, they are the focus of the following sections. Indeed, they will mainly

emphasis the way to obtain flexible, safe, smooth and attainable followers' set-points.

Furthermore, it is important to mention that the proposed MLMC architecture, embedded in each UGV, uses only set-points which are obtained with regard to only static or dynamic targets (defined by its current posture (position, orientation) and velocity)) [46], [59]. This allows, therefore, to avoid dealing with any rigid and specific path/trajectory planning. The main objective of this choice is to guarantee safe and flexible UGVs navigation since all the multi-UGVs planning and re-planning process manipulate only specific targets instead of complete trajectories which could be much more time-consuming and complex to make reasoning on them, to check, for instance, whether the MUGVs has conflict when navigating dynamically in cluttered environments [1].

#### IV. FORMATION MODELING AND CONTROL SET-POINTS

After an overview of the proposed MLMC architecture, let us focus on the formation modeling and on how to define the appropriate set-points to be followed by the multi-vehicle system. The main objective in controlling the navigation in formation of  $N$  UGVs consists on reaching and keeping any assigned geometrical shape, while guaranteeing safe, flexible and smooth reconfiguration between the different targeted shapes.

In what follows, an overview of formation strategy based on Cartesian reference frame (Rigid formation) and Frenet formation (Deformable formation) is first presented. Their advantages and drawbacks are discussed in subsection IV-A before to motivate and focus on the modeling and the formation set-points definition used in this paper (cf. Subsection IV-B).

##### A. Rigid vs. Deformable Formation Shape

The most intuitive formation definition consists of a Rigid Virtual Structure (RVS) [60] where each vertex of the RVS corresponds to a dynamic target (called secondary targets) to be tracked by one of the  $N$  vehicles in order to reach the desired geometrical formation. The formation dynamic is induced, at each sample time, by the current dynamic of the so-called main virtual target (cf. Figure 4). This main virtual target has generally constant geometric relations with each of the secondary targets, and its dynamic could be driven by centralized way [29], [37] or by the movement of a vehicle in the formation which will take the role of the leader [61], [62]. As given in Figure 4, this main virtual target is thus driven by an UGV of the fleet (which is called leader). An essential consideration to achieve *leader-follower* navigation of a group of UGVs, is that the followers must know, as accurately as possible, the leader's state (pose and velocity). The leader sends its state by reliable Wi-Fi communication (cf. Fig. 2). Nonetheless, cameras and/or LIDAR sensors embedded in each follower, can be used to estimate the leader's state [35], [63].

In the case of formation based on RVS, the leader dynamic should be constrained in order to maintain invariable the formation shape along the navigation (e.g., a triangle in Fig. 4).

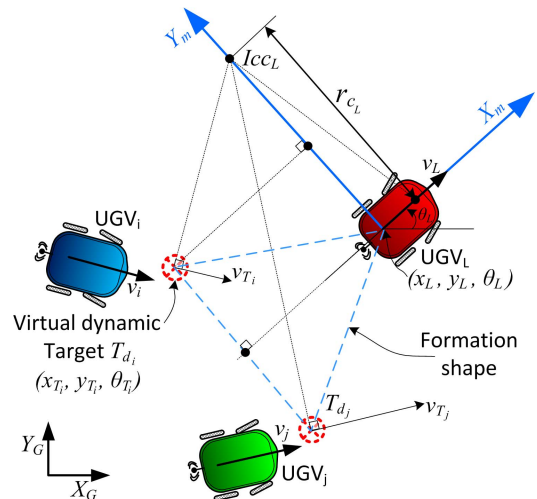


Fig. 4. Rigid Virtual Structure (RVS) based on Cartesian formation definition w.r.t. main virtual target.

Indeed, the position and orientation of each node (virtual target) are computed from the leader's configuration w.r.t. its local frame  $X_m Y_m$ . The idea behind this kind of formation is to eliminate the dependency of each UGV to a Global reference frame. The dynamic of this geometric structure is subordinated to the current dynamic of the leader [64]. The leader's position determines the nodes' positions according to the formation shape. The instantaneous center of curvature  $I_{ccL}$  of the formation is determined by the leader according to its movements (cf. Fig. 4).  $I_{ccL}$  allows to compute the desired orientation of the nodes according to the formation shape (cf. Fig. 4). The leader turns around  $I_{ccL}$  (positioned perpendicularly to its rear wheels), then the other target set-points  $T_{d_i}$  must also turn around  $I_{ccL}$  to maintain the rigid formation. Thus, the target velocity  $v_{T_i}$  at  $T_{d_i}$  must be tangent to the circle which has  $I_{ccL}$  as center. The advantage of RVS is that the followers require only instantaneous leader's configuration to determine its desired position in the formation [36]. Nevertheless, the leader velocity (linear and angular) has to be drastically constrained (thus the overall formation dynamic) in order that all the followers can satisfy their kinematic constraints, which is an important condition to have always steady formation navigation. An accurate analyze of these different leader constraints are discussed in [62].

In view of the important constraints imposed to the dynamic of the leader (thus, to the overall fleet) RVS is not used in the following developments. This paper focuses on a Deformable Virtual Structure (DVS), based on *leader-follower* strategy (cf. Fig. 5). It allows to each follower to navigate according to the trajectory trace of the leader, more specifically each follower is controlled longitudinally according to fixed curvilinear distance w.r.t. the current location of the leader and laterally, according to constant Euclidean distance w.r.t. the trajectory of the leader (cf. Fig. 5). The followers have thus to track the reference trajectory of the leader (or with an offset w.r.t. this trajectory) while ensuring to have always safe navigation along the road. It is to be noted that if a platooning

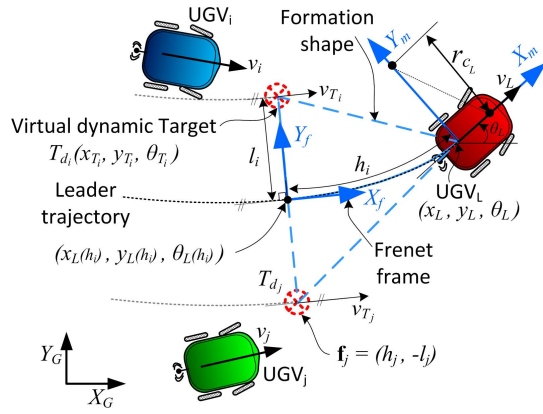


Fig. 5. Deformable Virtual Structure (DVS) based on Frenet reference frame linked to the leader's trajectory.

formation is performed [15] using this strategy (where the leader is ahead) then the followers are ensured, in static environment, to have always safe path to follow. Thus, the used formation is applied generally when tracking the leader's movements is more worthwhile than keeping an absolute rigid shape during the navigation. Nonetheless, while taking this last strategy, the geometric formation shape is distorted according to the reference path (cf. Section VI-B). The leader should also start its movement before to communicate its trajectory to other UGVs. Furthermore, the leader can also track a reference trajectory which is known beforehand by all the other UGVs. This kind of formation modeling could be used in several areas, such as: passengers' transportation or agriculture (cf. Section I).

### B. Set-Points Definition

In order to model the formation based on DVS, let us introduce some notations:

- A leader ( $UGV_L$  in Fig. 5); its pose  $(x_L, y_L, \theta_L)$ , its steering angle  $\gamma_L$  and its linear velocity  $v_L$  determine the dynamic of the formation (cf. Fig. 5).
- The formation structure is defined with as much nodes as necessary to obtain the desired formation shape. Each node  $i$  is a virtual dynamic target ( $T_{d_i}$ ). The formation is defined as  $\mathbf{F} = \{\mathbf{f}_i, i = 1 \dots N\}$ , where  $\mathbf{f}_i = (h_i, l_i)^T$  is the coordinates of the dynamic target  $T_{d_i}$  w.r.t. the leader's local reference frame (cf. Fig. 5).

An important characteristic of this formation definition, based on dynamic targets set-points, is the use of the heading  $\theta_T$  in addition to the target's positions  $(x_T, y_T)$ , which allows performing more accurate navigation in formation [29]. The followers have thus to track as accurately as possible these dynamic targets, without having to use any path or trajectory following/tracking control law [36], [37], which are more restrictive (accurate trajectory and vehicle pose) and less flexible (replanning in cluttered environment) and time consuming.

As mentioned above the formation set-points are obtained while knowing the leader's trajectory. Indeed, this trajectory is used to define the formation in longitudinal  $h_i$  (curvilinear)

and lateral  $l_i$  (perpendicular to the trajectory) Frenet coordinates [65] (cf. Fig. 5).

In the deformable formation, the pose of the virtual target  $T_{d_i}$  w.r.t. the leader's trajectory given in the Global reference frame can be written as:

$$\begin{bmatrix} x_{T_i} \\ y_{T_i} \\ \theta_{T_i} \end{bmatrix} = \begin{bmatrix} x_L(h_i) \\ y_L(h_i) \\ \theta_L(h_i) \end{bmatrix} + \begin{bmatrix} -l_i \sin(\theta_L(h_i)) \\ l_i \cos(\theta_L(h_i)) \\ 0 \end{bmatrix} \quad (2)$$

where  $(x_L(h_i), y_L(h_i), \theta_L(h_i))$  is the former leader's pose at  $h_i$  longitudinal distance from the current leader's pose along its trajectory (cf. Fig. 5). If  $h_i < 0$  then  $T_{d_i}$  is back to the current leader's pose. It is considered in the following developments that the leader starts its movements before other followers and it is always ahead of them at least for a curvilinear distance equal to  $h_i^d$  (cf. Fig. 5) in order to have all set-points available for all followers.

The coordinates  $h_i$  has to be constant to keep the desired curvilinear distance then, the follower's linear velocity at  $h_i$  along the leader's trajectory must be equal to the current linear velocity of the leader ( $v_L(h_i) = v_L$ ). When  $l_i \neq 0$ , the follower's velocity considers the leader's angular velocity  $\omega_L(h_i)$  to keep  $v_L$  at  $h_i$ . Moreover, the followers rotates with the same angular velocity  $\omega_L$  at  $h_i$ . The velocities of each  $T_{d_i}$  are given by:

$$v_{T_i} = v_L - l_i \omega_L(h_i) \quad (3)$$

$$\omega_{T_i} = \omega_L(h_i) = \frac{v_L}{r_{c_L}(h_i)} \quad (4)$$

where  $r_{c_L}(h_i)$  is the radius of curvature at  $h_i$  (longitudinal distance from the current leader's pose along its trajectory).

Next section describes the use of this set-points definition to change dynamically the formation configuration according to the environment context. The smooth changes between different formations shapes consider the inter-vehicle distance and vehicle kinematic constraints.

## V. STRATEGY FOR FORMATION RECONFIGURATION

Before to give the details of the proposed Strategy for Formation Reconfiguration (SFR), it is important to know how to manage the allocation of virtual targets to the followers UGVs. Different algorithms optimizing target assignment can be easily integrated in the proposed control architecture (cf. Fig. 2) [42], [43]. In this work, the allocation of virtual targets to UGVs is achieved using elementary rules when a formation reconfiguration is required (cf. Section VI for an example of scenario achieved with 3 actual UGVs). These rules assign a label  $H_i$  of the virtual target  $T_{d_i}$  to the  $UGV_i$  at the beginning of the experiment. This label is kept by each UGV along the reconfiguration process (cf. Fig. 6). Figure 7 shows the *Formation parameters* block of the control architecture for navigation in formation of a group of UGVs with dynamic reconfiguration according to the environment context.

The  $UGV_L$  (Leader) determines the desired formation shape according to the navigation context and can allows, for instance, to reconfigure the formation if any new obstacle or any narrow road is detected. Hence, according to this

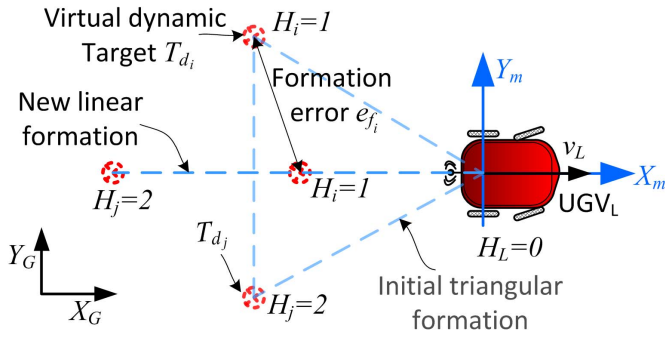


Fig. 6. Formation reconfiguration, for instance, from triangular to linear formation shapes based on inter-target distances.

desired formation shape and the current leader's configuration (cf. Fig. 7), the dynamic virtual targets  $T_{d_i}$  assigned to each follower is communicated by the leader (these virtual targets are transmitted to the followers while using *Communication* block shown in Fig. 2). The UGVs use also their range sensor to detect any unforeseen obstacle (cf. Fig. 7). In the case where they detect any too close, the proposed control architecture, embedded in each UGV, allows to have the capability to perform reactive obstacle avoidance (cf. Section III, Subsections III-B and III-C) [24], [53], [54].

In addition to the proposition of the overall MLMC architecture (cf. Section III) and the appropriate way to model the formation shape (based on dynamic targets set-points (cf. Section IV)), this paper proposes a new SFR, based on the definition of a suitable reconfiguration matrix (cf. Subsection V-B), of a group of UGVs. This strategy corresponds to the main contribution of this paper, it relies on the proposed MLMC structure in order to define an appropriate SFR guaranteeing the safety, smoothness and flexibility of the reconfiguration<sup>2</sup> of the MUGVs. The modeling and the stability analysis of the proposed reconfiguration strategy is emphasized in subsection V-A. Subsections V-B and V-C are dedicated to the analytic definition of the dynamic reconfiguration in order to ensure the integrity and the trajectory smoothness of all the UGVs composing the fleet. The proposed SFR allows us to use the proposed MLMC as fully reactive architecture, in the sense that the followers track the instantaneous state (pose and velocity) of the current assigned virtual targets (thus, without the use of any reference trajectory or any trajectory planning process).

#### A. SFR Modeling and Stability Analysis

The proposed SFR is an extension of [62]. It is used in this paper an appropriate stable and continuous functions (linking the initial targets' poses to their desired final poses) instead of the definition of specific decoupled progress of the targets' set-points and post-control of the UGVs velocities based on inter-vehicle distances (to avoid any collision, as given in [62]).

The proposed continuous function allows to have UGVs coupled progress, while ensuring safe and smooth fleet reconfiguration. This function is inspired on the Procrustes distance [66] which uses the distance errors between the vertex of

<sup>2</sup>Transition between the different steady formation of the fleet of vehicles.

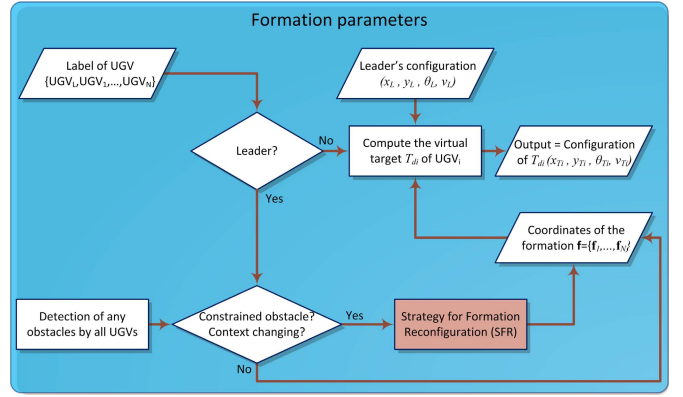


Fig. 7. Flowchart of the *Formation parameters* block for navigation in formation with dynamic reconfiguration.

the initial and new formation (cf. Fig. 6). Basically, the Procrustes distance  $P_d$  is a least-square type shape metric that require aligned shapes with one-to-one point correspondence.  $P_d$  is given by the square root of the summed squared difference between the positions of the vertex in two optimally superimposed configurations at centroid size [66]. The error between the coordinates of the current and new formations  $\mathbf{e}_{f_i}(e_{h_i}, e_{l_i})$  is defined as:

$$\mathbf{e}_{f_i}(t) = \mathbf{f}_i^n - \mathbf{f}_i(t) \quad (5)$$

where  $\mathbf{f}_i(h_i, l_i)$  and  $\mathbf{f}_i^n(h_i^n, l_i^n)$  are respectively the coordinates of the current and new desired formations (cf. Fig. 5 and 6). In order to guarantee the convergence to the new formation shape and smooth trajectories of the virtual target during the reconfiguration process, we propose to define adequately the time evolution of the derivative of  $\mathbf{e}_{f_i}$  as a function of the formation errors of all  $N$  virtual targets:

$$\dot{\mathbf{e}}_{f_i} = g(\mathbf{e}_{f_1}, \dots, \mathbf{e}_{f_i}, \dots, \mathbf{e}_{f_N}) \quad (6)$$

As we will see in the sequel, this formulation will allow to efficiently manage the minimum inter-target distance to avoid collisions between the followers while ensuring smooth targets' progress. The evolution of  $\mathbf{e}_{f_i}$  can be fixed by imposing a first order dynamic to (6):

$$\dot{\mathbf{e}}_f = \mathbf{A}\mathbf{e}_f \quad (7)$$

where  $\mathbf{e}_f = [\mathbf{e}_{f_1}, \dots, \mathbf{e}_{f_N}]^T$  and  $\mathbf{A}$  (called Reconfiguration Matrix) is a negative-definite matrix:

$$\mathbf{A} = \begin{bmatrix} a_{11} & a_{12} & \dots & a_{1N} \\ -a_{12} & a_{22} & \dots & a_{2N} \\ \vdots & \vdots & \ddots & \vdots \\ -a_{1N} & -a_{2N} & \dots & a_{NN} \end{bmatrix} \quad (8)$$

where  $a_i < 0$  with  $i = 1, \dots, N$  is related to the speed of convergence of the set-point error  $\mathbf{e}_{f_i}$  to reach the new formation, and  $a_{ij}$  with  $i \neq j$  is related to the inter-target distances between  $T_{d_i}$  and  $T_{d_j}$ . The values of the matrix entries must be designed while taking into account: the minimum inter-vehicles distance to avoid any collision (cf. Subsection V-B) and the kinematic constraints of the UGVs to allow

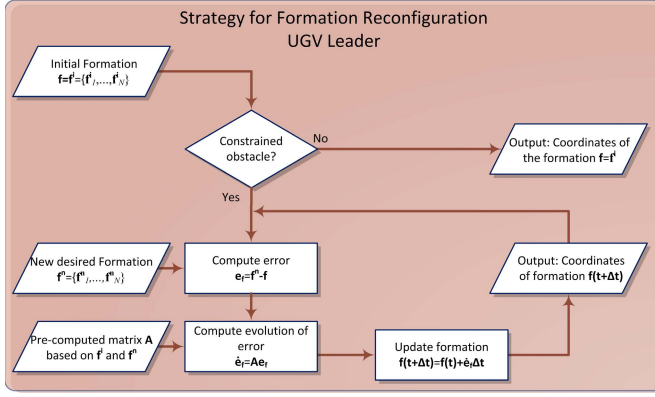


Fig. 8. Flowchart of the SFR block for dynamic reconfiguration of the set-points in the UGV leader (cf. Fig. 7).

each follower to track accurately its assigned target (cf. Subsection V-C).

Fig. 8 shows a block diagram of the SFR, the set-point error  $\mathbf{e}_{f_i}(t)$  is computed online, and using the reconfiguration matrix  $\mathbf{A}$  (pre-defined according to the desired new formation), the next error, represented in what follows by  $\mathbf{e}_{f_i}(t + \Delta t)$ , is obtained. Then, the new coordinates are updated until the error converges to zero.

The stability of the formation error system (7) can be straightforwardly proved using Lyapunov analysis [67]. Let us first define a Lyapunov candidate function as:

$$V = \frac{1}{2} \mathbf{e}_f^T \mathbf{e}_f \quad (9)$$

$V$  is a positive-definite function. To guarantee the stability of the system,  $\dot{V}$  must be negative-definite. By taking the derivative of eq. (9) and using (7),  $\dot{V}$  can be written:

$$\dot{V} = \mathbf{e}_f^T \dot{\mathbf{e}}_f \quad \mathbf{e}_f^T \mathbf{A} \mathbf{e}_f \quad (10)$$

Since  $\mathbf{A}$  is a negative-definite matrix (8), then  $\dot{V} < 0$  and the formation error system converge asymptotically. Nevertheless, it is not enough to highlight the stability of the formation error system given in eq. (7), it is primordial to appropriately define the matrix  $\mathbf{A}$  in order to guarantee any UGVs collisions. For that purpose, the following subsection is introduced.

### B. Reconfiguration Matrix Design

To avoid the collision between UGVs, the elements of matrix  $\mathbf{A}$  must be designed according to the allowed minimum distance between targets  $d_{Tmin}$  (to avoid collisions). It is to note that as shown in Fig. 3, each UGV is surrounded by a circle with a radius  $R_v$ , it is therefore enough to confirm that there is no collision between UGV to verify that the distance between all of them (during all their movements) will never be less than the sum of their radius plus a certain constant safety margin [58]. To determine the relation between the minimum distance  $d_{Tmin}$  and the elements of matrix  $\mathbf{A}$ , and for the sake of simplification to understand the proposed methodology, the case of two targets is defined and analyzed below (cf. Fig 9).

The inter-target distance can be computed as:

$$d_T^2 = \mathbf{e}_{f12}^T \mathbf{e}_{f12} \quad (11)$$

Furthermore, the inter-target error  $\mathbf{e}_{f12}$  can be written as:

$$\begin{aligned} \mathbf{e}_{f12} &= \mathbf{f}_1 - \mathbf{f}_2 \\ &= -\mathbf{f}_1^n + \mathbf{f}_1 + \mathbf{f}_2^n - \mathbf{f}_2 + \mathbf{f}_1^n - \mathbf{f}_2^n \\ &= -\mathbf{e}_{f1} + \mathbf{e}_{f2} + \mathbf{e}_{f12}^n \end{aligned} \quad (12)$$

Taking the derivative of eq. (11) to obtain its minimum value, we obtain:

$$\begin{aligned} \frac{\partial (d_T^2)}{\partial t} &= 0 \\ \frac{\partial (\mathbf{e}_{f12}^T \mathbf{e}_{f12})}{\partial t} &= \\ 2\mathbf{e}_{f12}^T \dot{\mathbf{e}}_{f12} &= \end{aligned} \quad (13)$$

Eq. (13) can be expressed using the derivative of eq. (12) and eq. (7) as follows:

$$\begin{aligned} \mathbf{e}_{f12}^T \dot{\mathbf{e}}_{f12} &= 0 \\ \mathbf{e}_{f12}^T [\dot{\mathbf{e}}_{f1} - \dot{\mathbf{e}}_{f2}] &= \\ \mathbf{e}_{f12}^T [(a_1 + a_{12})\mathbf{e}_{f1} + (a_{12} - a_2)\mathbf{e}_{f2}] &= \end{aligned} \quad (14)$$

Using eq. (12) in eq. (14), it is obtained:

$$\begin{aligned} \mathbf{e}_{f12}^T [(a_1 + a_{12})\mathbf{e}_{f1} + (a_{12} - a_2)(\mathbf{e}_{f1} + \mathbf{e}_{f12} - \mathbf{e}_{f12}^n)] &= 0 \\ \mathbf{e}_{f12}^T [(a_1 - a_2 + 2a_{12})\mathbf{e}_{f1} - (a_{12} - a_2)\mathbf{e}_{f12}^n] &= \\ - (a_{12} - a_2)\mathbf{e}_{f12}^T \mathbf{e}_{f12} &= \end{aligned} \quad (15)$$

Defining  $m_{12} = (a_1 - a_2 + 2a_{12}) / (a_2 - a_{12})$  and replacing it in eq. (15), it is obtained:

$$\begin{aligned} \mathbf{e}_{f12}^T [m_{12}\mathbf{e}_{f1} + \mathbf{e}_{f12}^n] - \mathbf{e}_{f12}^T \mathbf{e}_{f12} &= 0 \\ \mathbf{e}_{f12}^T [m_{12}\mathbf{e}_{f1} + \mathbf{e}_{f12}^n] &= \mathbf{e}_{f12}^T \mathbf{e}_{f12} \end{aligned} \quad (16)$$

Using the minimum distance between targets  $d_{Tmin}$  and eq. (11), then eq. (16) can be expressed as an inequality:

$$\begin{aligned} \mathbf{e}_{f12}^T [m_{12}\mathbf{e}_{f1} + \mathbf{e}_{f12}^n] &\geq \mathbf{e}_{f12min}^T \mathbf{e}_{f12min} \\ \mathbf{e}_{f12}^T [m_{12}\mathbf{e}_{f1} + \mathbf{e}_{f12}^n] &\geq d_{Tmin}^2 \end{aligned} \quad (17)$$

Analyzing the left side of eq. (17),  $|\mathbf{e}_{f12}|$  is the distance between target 1 and 2 eq. (11) and it must be greater than  $d_{Tmin}$  ( $|\mathbf{e}_{f12}| \geq d_{Tmin}$ ), then:

$$|m_{12}\mathbf{e}_{f1} + \mathbf{e}_{f12}^n| \geq d_{Tmin} \quad (18)$$

Eq. (18) shows the direct relation between  $m_{12}$  and  $d_{Tmin}$ , where the value of  $m_{12}$  is a function of  $a_1$ ,  $a_{12}$  and  $a_2$ . The values of  $a_1$ ,  $a_{12}$  and  $a_2$  have to be chosen to always satisfy (18). Moreover,  $a_1$ ,  $a_{12}$  and  $a_2$  are related to the variation  $\dot{\mathbf{f}}_i = (\dot{h}_i, \dot{l}_i)$ . Using the derivative of (5) and (7), we obtain:

$$\dot{\mathbf{e}}_{f1} = -\dot{\mathbf{f}}_1 = a_1 \mathbf{e}_{f1} + a_{12} \mathbf{e}_{f2} \quad (19)$$

$$\dot{\mathbf{e}}_{f2} = -\dot{\mathbf{f}}_2 = -a_{12} \mathbf{e}_{f1} + a_2 \mathbf{e}_{f2} \quad (20)$$

where  $\dot{\mathbf{f}}_i = (\dot{h}_i, \dot{l}_i)$ . Since  $h_i$  and  $l_i$  are directly related to the control inputs (velocities (3) and (4)), they should evolve to generate attainable virtual target's velocities

(cf. Subsection V-C). At this aim, we assume that  $\dot{h}_i$  and  $\dot{l}_i$  have to be less than the maximum vehicle's velocity and the values of  $a_1$ ,  $a_{12}$  and  $a_2$  must be selected considering that  $a_i \ll v_{max}$ .

Fig. 9(a) shows this case of two targets and the leader w.r.t. the Global and local leader's reference frame, a triangular formation is reshaped, two vertex of the formation switch between them and inter-distance is reduced from 2 m to 1 m (cf. Fig. 9(a)). For  $d_{Tmin} = 0.5$  m, the designed values are  $m_{12} = 1$ ,  $a_1 = -0.5$  and  $a_2 = -1$ . The value of  $a_{12} = -0.5$  is obtained using the definition of  $m_{12}$ . The smooth evolution of the coordinates  $\mathbf{f}_i = (h_i, l_i)$  of each target and their convergence to the new coordinates  $\mathbf{f}_i^t$  are shown in Fig. 9(b). It can be observed that the target  $T_{d2}$  goes back w.r.t. the leader reference frame. This action is due to the deceleration of  $T_{d2}$  in order to reach its final position w.r.t. Global reference frame. Fig. 9(c) shows the distances between all the targets during the reconfiguration process. It can be noted that these designed values of the reconfiguration matrix (17) satisfy the minimum inter-target distances guaranteeing non inter-UGVs collisions.

### C. Formation Constraints

The formation constraints are related to analyze the relation between the formation coordinates  $\mathbf{f}_i(h_i, l_i)$  and the vehicle's kinematic constraints. Large values of  $\mathbf{f}_i$  can lead to the saturation of the commands in order to attain large set-point velocities. The tracked virtual target becomes thus unattainable, inducing at the end a lost or unreachable formation. In order to generate "attainable virtual targets" of each follower during the navigation and reconfiguration, the dynamic of the deformable formation is analyzed according to the kinematic limits of the used UGVs. It depends mainly on the reference trajectory (leader's trajectory) eq. (2), (3) and (4). This trajectory is represented in Frenet frame (curvilinear distance and radius of curvature) while the followers' constraints are given by  $v_{max}$  and  $r_{cmin}$ . The velocities and radius of curvature of the followers are constrained by

$$|v_{T_i}| \leq v_{max} \quad (21)$$

$$r_{cmin} \leq |v_{T_i} \omega_{T_i}^{-1}| \quad (22)$$

Eq. (21) and (22) can be expressed as a function of leader's velocity using eq. (3) and (4) as follows:

$$|v_L - l_i \omega_L(h_i)| \leq v_{max} \quad (23)$$

$$r_{cmin} \leq |v_L \omega_{T_i}^{-1} - l_i \omega_L(h_i) \omega_{T_i}^{-1}| \quad (24)$$

Replacing  $\omega_{T_i} = \omega_L(h_i) = v_L r_{cL}^{-1}(h_m)$  in eq. (23) and (24), we obtain:

$$|v_L - v_L l_i r_{cL}^{-1}(h_m)| \leq v_{max} \quad (25)$$

$$r_{cmin} \leq |r_{cL}(h_m) - l_i| \quad (26)$$

We define  $\mathbf{f}_m = (h_m, l_m)^T$  as the coordinates of the farthest node. The maximum of the absolute value of eq. (25) occurs when  $l_i = -l_m$  and  $r_{cL} = r_{cmin}$ . In eq. (26), the minimum value of the absolute value occurs when  $l_i = l_m$ . The leader's

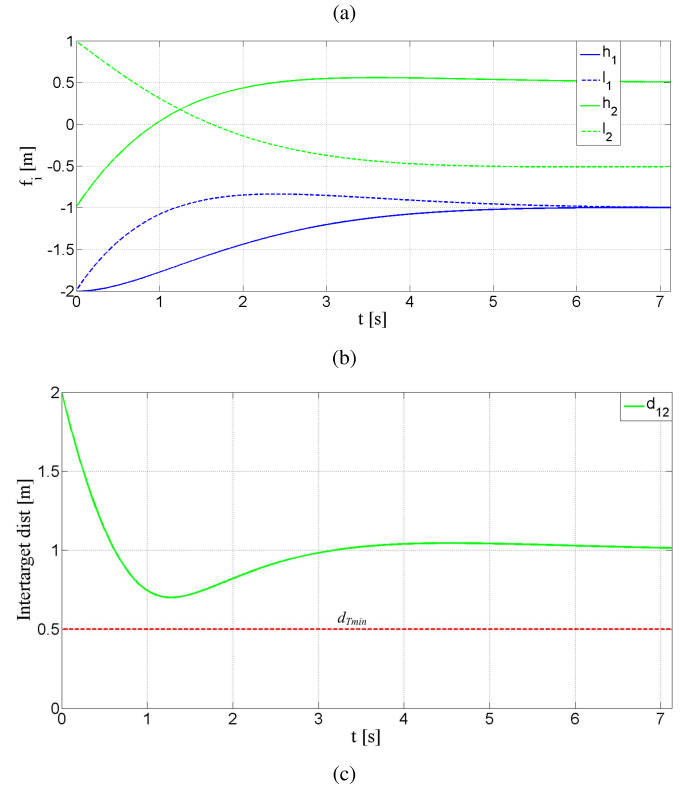
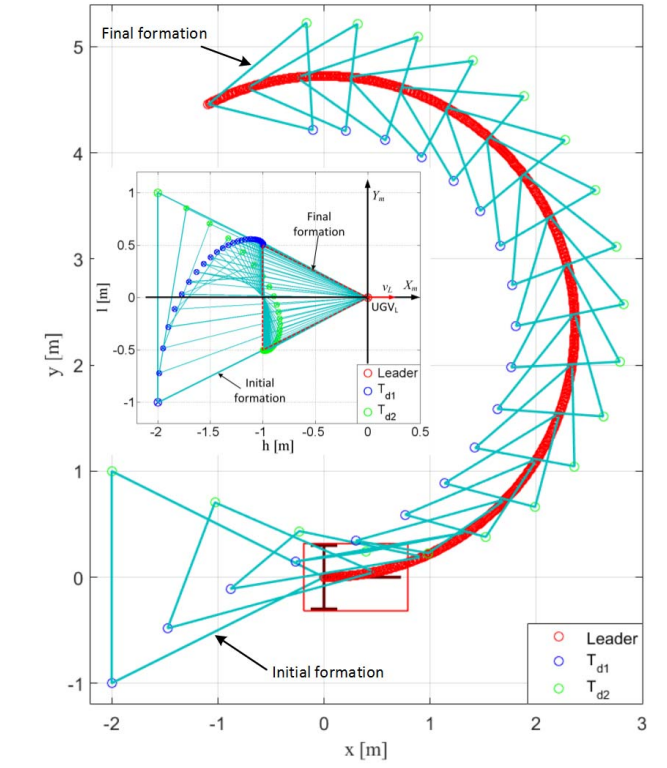


Fig. 9. Example of proposed SFR applied to triangle formation of  $N = 2$  virtual targets and the leader. (a) Evolution of SFR w.r.t. the Global and leader's references frame. (b) Progress of the coordinates  $\mathbf{f}_i = (h_i, l_i)$  of each target. (c) Inter-target distance.

linear velocity can be written as:

$$v_L(1 - l_m r_{cmin}^{-1}) \leq v_{max} \quad (27)$$

$$v_L \leq v_{max}(1 - l_m r_{cmin}^{-1})^{-1}$$

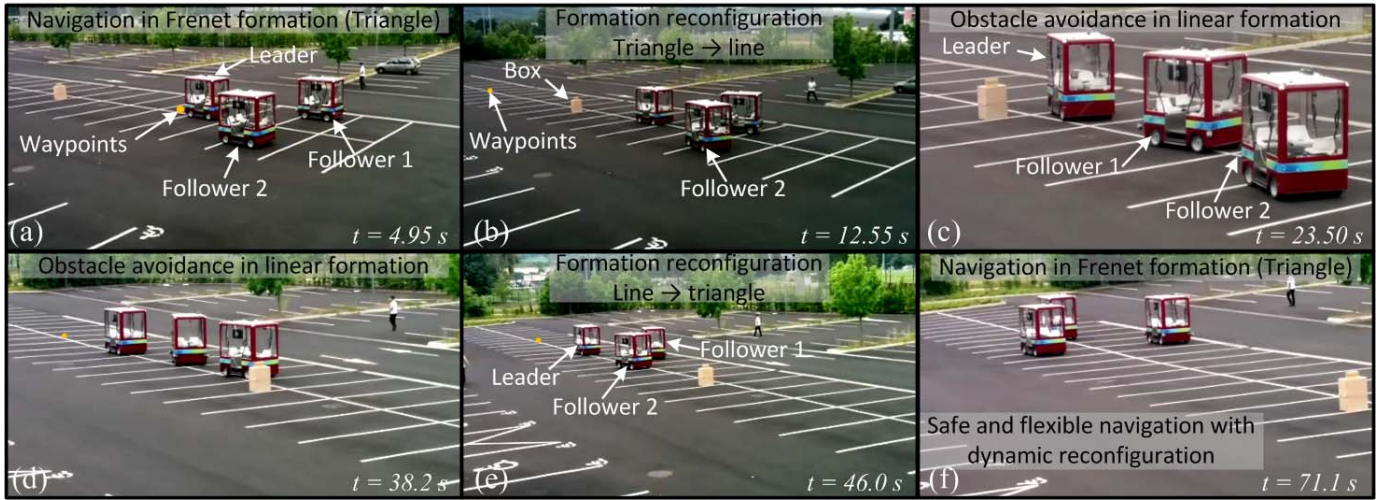


Fig. 10. Navigation of  $N = 3$  UGVs performing reconfiguration of the formation using the SFR.

Moreover, the leader's radius of curvature can be written:

$$\begin{aligned} r_{c_{min}} &< r_{c_L}(h_m) - l_m \\ r_{c_{min}} + l_m &< r_{c_L}(h_m) \end{aligned} \quad (28)$$

It can be noted that the linear velocity  $v_L$  and the radius of curvature  $r_{c_L}$  of the leader are constrained mainly according to the lateral coordinate of the formation  $l_m$  (eq. (27) and (28)). The linear velocity at  $h_i^f$  (curvilinear distance) and  $l_i^f = 0$  is equal to the current linear velocity of the leader which allows to keep constant the curvilinear distance.

Finally, from eq. (27) and (28), the leader's constraints of  $v_{Lmax}$  and  $r_{c_{Lmin}}$  are obtained.

$$v_{Lmax} = v_{max}(1 - l_m r_{c_{min}}^{-1})^{-1} \quad (29)$$

$$r_{c_{Lmin}} = r_{c_{min}} + l_m \quad (30)$$

These leader's constraints (velocity and radius of curvature) must be respected along all its movements in order to guarantee the respect of the follower kinematic constraints. This means that the leader has to limit its velocities to permit to the followers to reach actually their assigned targets, and thus to obtain and to keep the suitable formation shape.

## VI. EXPERIMENTAL VALIDATION

The objective of this experiment is to validate the proposed strategy for formation reconfiguration based on inter-target distance matrix between two deformable formation configurations (triangular and linear shapes) while navigating in a cluttered environment. This experiment has been done while using three electrical vehicles (cf. Fig. 10). This experiment can be found online.<sup>3</sup>

### A. Testbed and Scenario

The electrical urban vehicle VIPALAB (*Véhicule Individuel Public et Autonome pour LABoratoire*) is used in our experiments. This vehicle carries different embedded proprioceptive

TABLE I  
VIPALAB PLATFORM

VIPALAB	Elements	Description
	Chassis	(l,w,h)=(1.96, 1.30, 2.11) m
	Weight	400 kg (without batteries)
	Motor	Triphase 3x28 V, 4 KW
	Break	Integrated to the motor
	Max. speed	20 km/h ( $\approx 5.5$ m/s)
	Batteries	8 batteries 12 V, 80 Ah
	Autonomy	3 hours at full charge
	Computer	Intel Core i7, CPU:1.73 GHz RAM:8GB, OS:Ubuntu12.04

and exteroceptive sensors such as cameras, odometers, IMUs, steering angle sensor, an RTK-GPS, a Wi-Fi communication system and a computer. Some specifications of VIPALAB are shown in Table I (more details are given in [68]). Each vehicle uses a combination of RTK-GPS and IMU to estimate its current position and orientation at a sample time of  $T_s = 0.1$  s (cf. Table I). Indeed, in these experiments, the vehicles move at maximum velocity of  $2.5$  m/s and the minimum radius of curvature  $r_{c_{min}} = 2.83$  m (cf. Fig. 10) and the Wi-Fi communication system is stable between VIPALABs. Each VIPALAB can be controlled using the on-board computer (through CAN protocol) or a wired control panel attached to the vehicle.

In the prospect of future deployment of the proposed MLMC architecture in urban environments, it is essential to take into account the UGVs' communication, perception and localization features [1, Ch. 1]. Indeed, even if these topics are outside the immediate scope of the paper, it is highlighted below the main concerns impacting the proposed cooperative navigation in formation. First of all, it is important to have robust and steady V2V (vehicle-to-vehicle) wireless communication [2]. This is particularly true for high speed vehicles (in highway for instance [4]) where the communication Quality of Service (such as: transmission delay/latency, bandwidth, level of the error rate, etc.) has a significant impact on the safety and

<sup>3</sup><https://youtu.be/ZXOjEUZ-VIY>

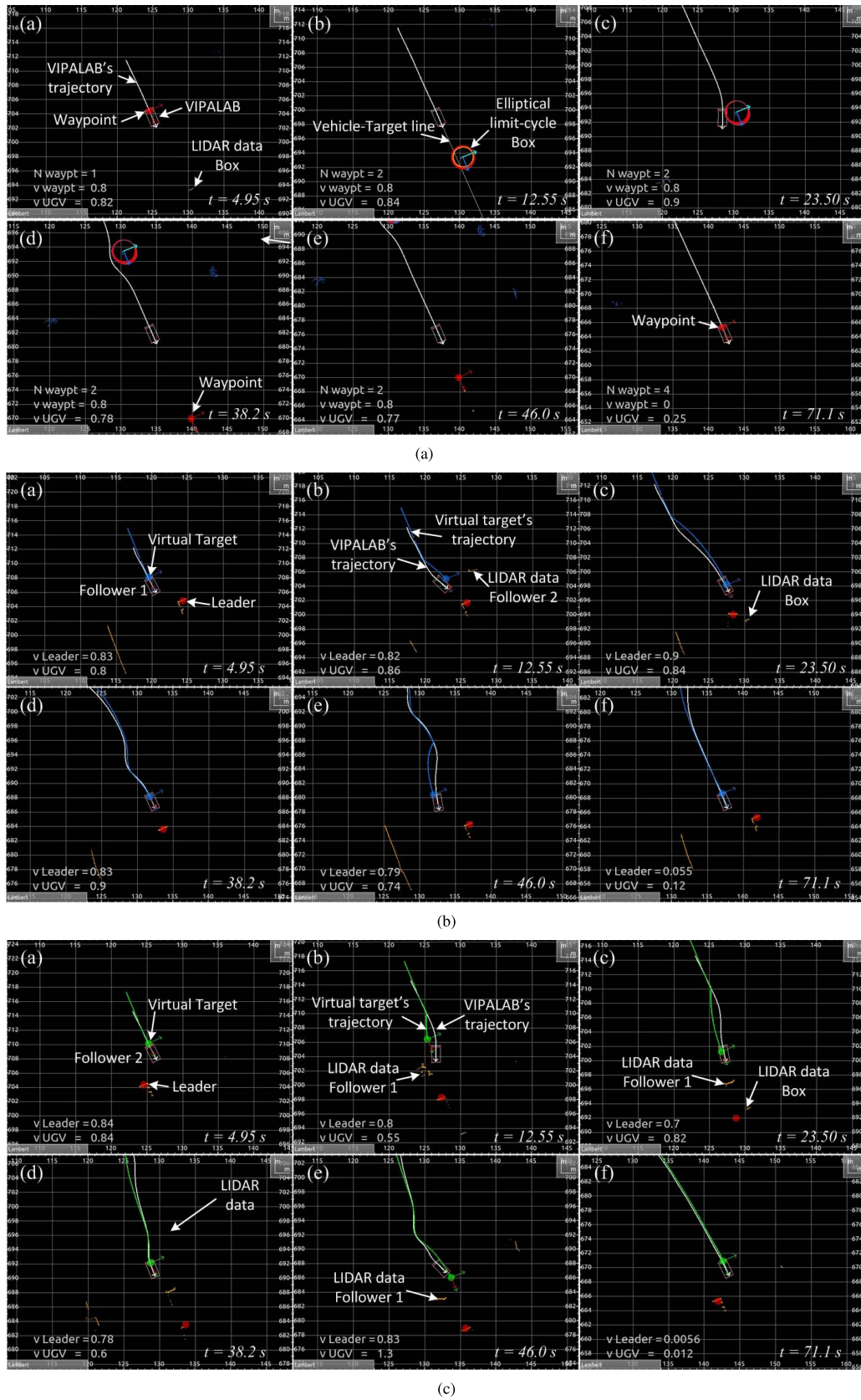


Fig. 11. Validation of the navigation with reconfiguration using the SFR in deformable formation for a group of  $N = 3$  UGVs. (a) Leader (“v UGV” and “v waypoint” are respectively the current velocities of the UGV and the “N waypoint”). (b) Follower 1 (“v UGV” and “v Leader” are respectively the follower’s and the leader’s current velocities). (c) Follower 2 (“v UGV” and “v Leader” are respectively the follower’s and the leader’s current velocities).

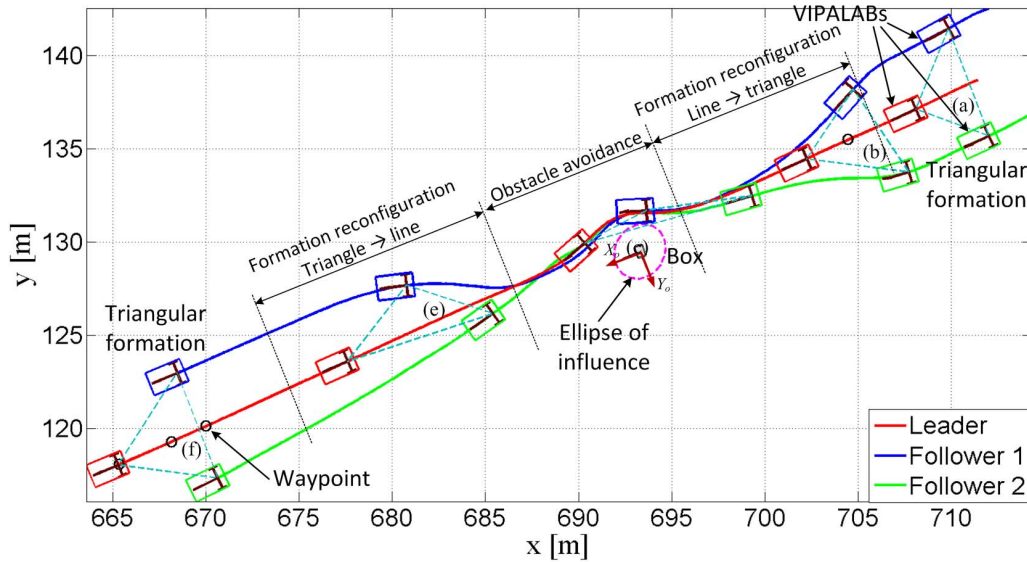


Fig. 12. Vehicles' trajectories using the SFR.

controllability of the multi-UGV system. The wireless security face to external intrusion / hacking is also among the main concerns of such connected vehicles [69]. Secondly, in terms of UGV's perceptions, the two main features which should be available and robust in the used UGVs are: appropriate functionalities to detect the navigable area (delimited generally by pavements and/or ground painting) [70]; and dynamic obstacle detection and characterization [71]. Thirdly, since the fleet of UGVs needs to know as precisely as possible their mutual localization in the environment, it is also important to have reliable and guaranteed GPS information. In urban area, the GPS reception could be very poor, due for instance to street canyons [72], nevertheless several alternatives exist to obtain precise localization, for instance by using cameras or/and 3D-LIDARs [73]. One of the main future extensions of the proposed MLMC architecture is to take into account explicitly the failure/uncertainties related to the communication as well as the perception/localization modules in the planning and the control process to always guarantee the integrity of the controlled vehicles.

### B. Experimental Results

In this experiment the leader of the group of VIPALABs has to reach successively static set of waypoints, presented in [59], and the followers has to keep the desired formation, defined according to the leader's position and velocity (cf. Subsection IV-B), while avoiding the obstacles. The leader's configuration is sent by itself to each follower via Wi-Fi. At this aim, each follower tracks its assigned dynamic virtual target (cf. Fig. 11(b) and 11(c)) applying the control law, proposed in [46], to the multi-robot system. The initial followers' positions w.r.t. the leader's position are  $(\Delta x, \Delta y) = (-6, \pm 3) m$  according to the Global reference frame.

The initial formation coordinates are defined by  $\mathbf{F}^i = (\mathbf{f}_1^i, \mathbf{f}_2^i)$ , with  $\mathbf{f}_1^i = (-5, -3)^T m$  and  $\mathbf{f}_2^i = (-5, 3)^T m$  (triangular shape). A set of waypoints is defined in the environment,

the leader (and thus the formation) must go toward them while avoiding obstacles. The new targeted formation is defined as straight line with the following coordinates  $\mathbf{F}^n = (\mathbf{f}_1^n, \mathbf{f}_2^n)$ , with  $\mathbf{f}_1^n = (-5, 0)^T m$  and  $\mathbf{f}_2^n = (-10, 0)^T m$ . The values of the matrix  $\mathbf{A}$  for the formation reconfiguration was designed according to the  $d_{Tmin} = 2.0 m$  and  $v_{max} = 2.5 m/s$ , they are given by:

$$\mathbf{A} = \begin{bmatrix} -0.114 & 0.018 \\ -0.018 & -0.143 \end{bmatrix} \quad (31)$$

Figure 10 shows the sequence of the multi-robot evolution, from the beginning of navigation with initial triangular formation  $\mathbf{F}^i$  to linear one  $\mathbf{F}^n$ , when the leader detects an obstacle (with adequate range to allow the formation reconfiguration), and once the last follower detects the end of the obstacle, the formation return to triangular formation.

Some screen-shots of the developed Graphical Data Interface for VIPALAB (GDI-VIPA) of the leader and followers are shown in Fig. 11(a), 11(b) and 11(c). In the leader's GDI-VIPA, the white line represents UGV's trajectory, the orange points are the set of waypoints and the big red point is the current assigned waypoint. It can be noted that the online detection of the box using the LIDAR sensor [54] and the reactive obstacle avoidance (based on elliptical limit-cycle [53], [54] (cf. Subsection III-B)) performed by the UGV (cf. Fig. 11(a) (b), (c) and (d)). This paper focuses on the navigation in formation, the leader's analysis (navigation through waypoints and reactive obstacle avoidance) was done in [46] and [59].

In the follower's GDI-VIPA (cf. Fig. 11(b) and 11(c)), the red point is the current leader's pose and the blue and green points are respectively the current virtual target to be tracked by follower 1 and 2. Therefore, the followers track their virtual targets to keep the desired deformable formation  $\mathbf{F}$  even during the reconfiguration phase (cf. Fig. 10 and Fig. 12).

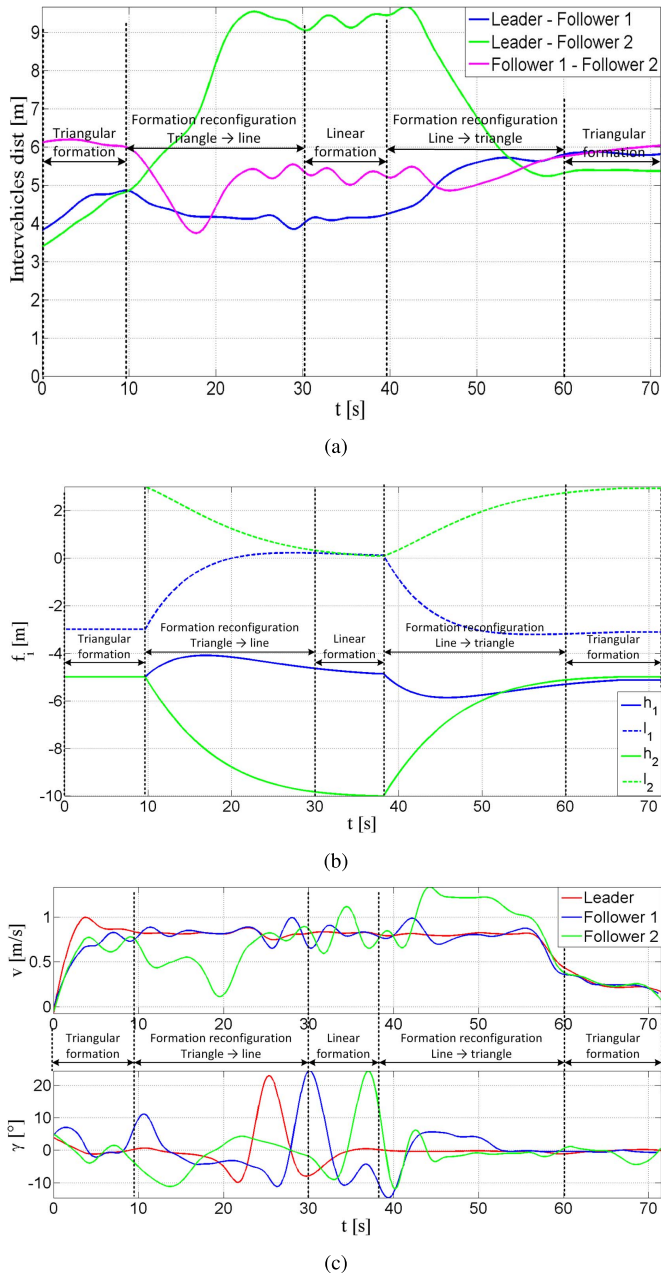


Fig. 13. Experimental results of the navigation with reconfiguration (SFR). (a) Distance among the UGVs. (b) Progress of the set-point definition  $f_i$  according to the SFR. (c) Commands (velocity and steering angle) of each UGV.

Figure 12 shows safe and smooth trajectories of the group of VIPALABs. It can be observed that the vehicles' trajectories are stables and the followers converge to their assigned virtual dynamic target even during the reconfiguration phase. Therefore, the desired formation, triangle (no obstacles) or line (during obstacle avoidance), is attained and kept. Fig. 13(a) shows the distance between each UGV of the formation. This last figure shows clearly the non-collision between the vehicles in the formation. Fig. 13(b) shows the evolution of the formation coordinates ( $h_i, l_i$ ) (virtual target positions) w.r.t. the leader. It can be observed smooth evolution of the formation coordinates (7) which attest on the efficiency of the strategy for formation reconfiguration.

Fig. 13(c) shows the velocity and steering angle of the vehicles. The reconfiguration strategy was designed to reduce the peaks of the control commands of each UGV when the transitions between the formation occur (cf. Subsection V-C). It can be noted that the commands are smooth and satisfy the kinematic vehicle's constraint ( $v_{max} = 2.5$  m/s and  $r_{cmin} = 2.83$  m) (cf. Subsection V-C).

Therefore, a smooth, flexible and safe trajectories for the multi-robot navigation in formation were obtained. The proposed control architecture allows also to adapt the formation configuration according to the environment context.

## VII. CONCLUSION

This paper proposed a complete and a modular Multi-Layer and Multi-Controller (MLMC) architecture for dynamic navigation in formation of a group UGVs in constrained environments. This architecture, based on *leader-follower* and *behavior-based* approaches, ensures reliable and stable navigation of a fleet of UGVs, performing several dynamic shape configurations and re-configurations. It allows us to ensure the safety, smoothness and flexibility of the overall fleet navigation. The formation shape and its progress over the time are defined according to appropriate dynamic targets set-points, which depend on the leader's state (pose and velocity) and the targeted formation shape. First, the paper has made the focus on several *leader-follower* formation definitions, based on Rigid or Deformable Virtual Structure (named respectively RVS and DVS). In the RVS, the leader's reference trajectory is not taken into account such as in DVS, only its current pose and dynamic has to be known by the followers. Furthermore, after giving their main advantages and drawbacks, the DVS has been chosen to be the basis of modeling and control of the fleet of vehicles. Secondly, and it is the main contribution of the paper, it is proposed in order to deal with dynamic shape reconfiguration of the fleet, a stable and online Strategy of Formation Reconfiguration (SFR) applied to the DVS. The asymptotic stability (based on Lyapunov synthesis) and the safety (avoiding any inter-vehicle collisions) demonstration of the fleet reconfiguration relies mainly on an analytic definition of an appropriate Reconfiguration Matrix  $A$ . This matrix takes into account the initial and the desired formation shapes/parameters; and guarantee that the progress of the vehicles' set-points are always smooth and that the vehicles' inter-distances are always above an authorized minimum distance. In addition, while proposing an analytic formulation of the leader's kinematic constraints (maximum linear and angular velocities) according to the current overall fleet state and constraints, the followers are always ensured to reach asymptotically and keeping their assigned virtual targets (and thus the formation). The proposed SFR can be applied for different situations when the formation has to be modified according to the environment context (dynamic, cluttered, etc.). Simulations and experiments using several UGVs have shown the reliability, efficiency and flexibility of the proposed strategy for multi-UGVs navigation and dynamic reconfiguration in constrained environments. The proposed MLMC architecture has been embedded in each

UGV (belong the group of the used autonomous electric vehicles) and shows the reliability of the different proposals. In future works, formation reconfiguration strategy even in highly uncertain environments (for instance, w.r.t. the vehicle's communication/perception/localization) will be addressed.

## REFERENCES

- [1] L. Adouane, *Autonomous Vehicle Navigation: From Behavioral to Hybrid Multi-Controller Architectures*. Boca Raton, FL, USA: CRC Press, Apr. 2016, p. 228.
- [2] D. Jia, K. Lu, J. Wang, X. Zhang, and X. Shen, "A survey on platoon-based vehicular cyber-physical systems," *IEEE Commun. Surveys Tuts.*, vol. 18, no. 1, pp. 263–284, 1st Quart., 2016.
- [3] J. Levinson and S. Thrun, "Robust vehicle localization in urban environments using probabilistic maps," in *Proc. IEEE Int. Conf. Robot. Automat.*, Anchorage, AK, USA, May 2010, pp. 4372–4378.
- [4] K. C. Dey *et al.*, "A review of communication, driver characteristics, and controls aspects of cooperative adaptive cruise control (CACC)," *IEEE Trans. Intell. Transp. Syst.*, vol. 17, no. 2, pp. 491–509, Feb. 2016.
- [5] V. Digani, L. Sabattini, C. Secchi, and C. Fantuzzi, "Ensemble coordination approach in multi-AGV systems applied to industrial warehouses," *IEEE Trans. Autom. Sci. Eng.*, vol. 12, no. 3, pp. 922–934, Jul. 2015.
- [6] L. Emmi, M. Gonzalez-de-Soto, G. Pajares, and P. Gonzalez-de-Santos, "New trends in robotics for agriculture: Integration and assessment of a real fleet of robots," *Sci. World J.*, vol. 2014, p. 21, Mar. 2014.
- [7] R. M. Murray, "Recent research in cooperative control of multivehicle systems," *J. Dyn. Syst., Meas., Control*, vol. 129, no. 5, pp. 571–583, 2007.
- [8] S. Knorn, Z. Chen, and R. H. Middleton, "Overview: Collective control of multiagent systems," *IEEE Trans. Control Netw. Syst.*, vol. 3, no. 4, pp. 334–347, Dec. 2016.
- [9] J. Liu, B.-G. Cai, and J. Wang, "Cooperative localization of connected vehicles: Integrating GNSS with DSRC using a robust cubature Kalman filter," *IEEE Trans. Intell. Transp. Syst.*, vol. 18, no. 8, pp. 2111–2125, Aug. 2017.
- [10] A. Bazzi, B. M. Masini, A. Zanella, and I. Thibault, "On the performance of IEEE 802.11p and LTE-V2V for the cooperative awareness of connected vehicles," *IEEE Trans. Veh. Technol.*, vol. 66, no. 11, pp. 10419–10432, Nov. 2017.
- [11] D. Song, R. Tharmarasa, T. Kirubarajan, and X. N. Fernando, "Multi-vehicle tracking with road maps and car-following models," *IEEE Trans. Intell. Transp. Syst.*, vol. 19, no. 5, pp. 1375–1386, May 2018.
- [12] S. Thrun. (2011). How Google's self-driving car works. IEEE Spectrum. [Online]. Available: <http://spectrum.ieee.org/automaton/robotics/artificial-intelligence/how-google-self-driving-car-works>
- [13] (2012). *Safe Road Trains for the Environment*. Accessed: Jan. 2018. [Online]. Available: [http://cordis.europa.eu/project/rcn/92577\\_fr.html](http://cordis.europa.eu/project/rcn/92577_fr.html)
- [14] (2016). *Grand Cooperative Driving Challenge*. Accessed: Jan. 2018. [Online]. Available: <http://www.gcdc.net/>
- [15] P. Avanzini, B. Thuilot, and P. Martinet, "Urban vehicle platoon using monocular vision: Scale factor estimation," in *Proc. 11th Int. Conf. Control, Automat., Robot. Vis.*, Singapore, Dec. 2010, pp. 1803–1808.
- [16] X. Guo, J. Wang, F. Liao, and R. S. H. Teo, "Distributed adaptive integrated-sliding-mode controller synthesis for string stability of vehicle platoons," *IEEE Trans. Intell. Transp. Syst.*, vol. 17, no. 9, pp. 2419–2429, Sep. 2016.
- [17] A. J. Häusler, A. Saccon, A. P. Aguiar, J. Hauser, and A. M. Pascoal, "Energy-optimal motion planning for multiple robotic vehicles with collision avoidance," *IEEE Trans. Control Syst. Technol.*, vol. 24, no. 3, pp. 867–883, May 2016.
- [18] S. Tsugawa, S. Jeschke, and S. E. Shladover, "A review of truck platooning projects for energy savings," *IEEE Trans. Intell. Veh.*, vol. 1, no. 1, pp. 68–77, Mar. 2016.
- [19] R. Rajamani, H.-S. Tan, B. K. Law, and W.-B. Zhang, "Demonstration of integrated longitudinal and lateral control for the operation of automated vehicles in platoons," *IEEE Trans. Control Syst. Technol.*, vol. 8, no. 4, pp. 695–708, Jul. 2000.
- [20] R. Horowitz and P. Varaiya, "Control design of an automated highway system," *Proc. IEEE*, vol. 88, no. 7, pp. 913–925, Jul. 2000.
- [21] Y. U. Cao, A. S. Fukunaga, and A. B. Kahng, "Cooperative mobile robotics: Antecedents and directions," *Auton. Robots*, vol. 4, no. 1, pp. 7–27, 1997.
- [22] H. Jones and M. Snyder, "Supervisory control of multiple robots based on a real-time strategy game interaction paradigm," in *Proc. IEEE Int. Conf. Syst., Man Cybern. e-Syst. e-Man Cybern. Cyberspace*, Oct. 2001, pp. 383–388.
- [23] T. Fukuda, I. Takagawa, K. Sekiyama, and Y. Hasegawa, "Hybrid approach of centralized control and distributed control for flexible transfer system," in *Distributed Manipulation*. Norwell, MA, USA: Kluwer, 2000, pp. 65–85, doi: [10.1007/978-1-4615-4545-3\\_4](https://doi.org/10.1007/978-1-4615-4545-3_4).
- [24] L. Adouane, "Reactive versus cognitive vehicle navigation based on optimal local and global PELC," *Robot. Auton. Syst.*, vol. 88, pp. 51–70, Feb. 2017.
- [25] E. Gat, "Three-layer architectures," in *Artificial Intelligence and Mobile Robots*, R. B. D. Kortenkamp and R. Murphy, Eds. AAAI Press, 1998, pp. 195–210.
- [26] H. C. H. Hsu and A. Liu, "A flexible architecture for navigation control of a mobile robot," *IEEE Trans. Syst., Man, Cybern. A, Syst. Humans*, vol. 37, no. 3, pp. 310–318, May 2007.
- [27] L. Adouane, "Toward smooth and stable reactive mobile robot navigation using on-line control set-points," in *Proc. IEEE/RSJ IROS, 5th Workshop Planning, Perception Navigat. Intell. Vehicles*, Tokyo, Japan, Nov. 2013, pp. 1–6.
- [28] H. Tang, A. Song, and X. Zhang, "Hybrid behavior coordination mechanism for navigation of reconnaissance robot," in *Proc. IEEE/RSJ Int. Conf. Intell. Robots Syst.*, Oct. 2006, pp. 1773–1778.
- [29] A. Benzerrouk, L. Adouane, and P. Martinet, "Stable navigation in formation for a multi-robot system based on a constrained virtual structure," *Robot. Auton. Syst.*, vol. 62, no. 12, pp. 1806–1815, 2014.
- [30] J. Vilca, L. Adouane, and Y. Mezouar, "Adaptive leader-follower formation in cluttered environment using dynamic target reconfiguration," in *Distributed Autonomous Robotic Systems*. Tokyo, Japan: Springer, 2016, pp. 237–254.
- [31] T. Balch and R. C. Arkin, "Behavior-based formation control for multirobot teams," *IEEE Trans. Robot. Autom.*, vol. 14, no. 6, pp. 926–939, Dec. 1998.
- [32] C.-F. Chang and L.-C. Fu, "A formation control framework based on Lyapunov approach," in *Proc. IEEE/RSJ Int. Conf. Intell. Robots Syst.*, Sep. 2008, pp. 2777–2782.
- [33] Z. Chao, S.-L. Zhou, L. Ming, and W.-G. Zhang, "UAV formation flight based on nonlinear model predictive control," *Math. Problems Eng.*, vol. 2012, pp. 1–15, 2012.
- [34] S.-M. Lee, H. Kim, H. Myung, and X. Yao, "Cooperative coevolutionary algorithm-based model predictive control guaranteeing stability of multi-robot formation," *IEEE Trans. Control Syst. Technol.*, vol. 23, no. 1, pp. 37–51, Jan. 2015.
- [35] A. K. Das, R. Fierro, V. Kumar, J. P. Ostrowski, J. Spletzer, and C. J. Taylor, "A vision-based formation control framework," *IEEE Trans. Robot. Autom.*, vol. 18, no. 5, pp. 813–825, Oct. 2002.
- [36] X. Chen and Y. Li, "Smooth formation navigation of multiple mobile robots for avoiding moving obstacles," *Int. J. Control, Automat., Syst.*, vol. 4, no. 4, pp. 466–479, 2006.
- [37] I. Shames, M. Deghat, and B. D. O. Anderson, "Safe formation control with obstacle avoidance," in *Proc. 18th IFAC World Congr.*, Milan, Italy, 2011, pp. 11252–11257.
- [38] L. Krick, M. E. Broucke, and B. A. Francis, "Stabilisation of infinitesimally rigid formations of multi-robot networks," *Int. J. Control*, vol. 82, no. 3, pp. 423–439, 2009, doi: [10.1080/00207170802108441](https://doi.org/10.1080/00207170802108441).
- [39] M. Lemay, F. Michaud, D. Letourneau, and J.-M. Valin, "Autonomous initialization of robot formations," in *Proc. IEEE Int. Conf. Robot. Automat. (ICRA)*, vol. 3, Apr./May 2004, pp. 3018–3023.
- [40] S. Halle, J. Laumonier, and B. Chaib-Draa, "A decentralized approach to collaborative driving coordination," in *Proc. 7th Int. IEEE Conf. Intell. Transp. Syst.*, Oct. 2004, pp. 453–458.
- [41] T. Sakaguchi, A. Uno, S. Kato, and S. Tsugawa, "Cooperative driving of automated vehicles with inter-vehicle communications," in *Proc. IEEE Intell. Vehicles Symp.*, Oct. 2000, pp. 516–521.
- [42] A. Benzerrouk, L. Adouane, and P. Martinet, "Altruistic distributed target allocation for stable navigation in formation of multi-robot system," in *Proc. 10th Int. IFAC Symp. Robot Control (SYROCO)*, Dubrovnik, Croatia, Sep. 2012, pp. 676–681.
- [43] F. Debbat and L. Adouane, "Formation control and role assignment of autonomous mobile robots in unstructured environment," *J. Control Intell. Syst.*, vol. 44, no. 2, 2016.
- [44] F. Li, Y. Ding, M. Zhou, K. Hao, and L. Chen, "An affection-based dynamic leader selection model for formation control in multirobot systems," *IEEE Trans. Syst., Man, Cybern., Syst.*, vol. 47, no. 7, pp. 1217–1228, Jul. 2017.

- [45] L. Adouane, "Hybrid and safe control architecture for mobile robot navigation," in *Proc. 9th Conf. Auton. Robot Syst. Competitions*, Castelo Branco, Portugal, May 2009.
- [46] J. Vilca, L. Adouane, and Y. Mezouar, "A novel safe and flexible control strategy based on target reaching for the navigation of urban vehicles," *Robot. Auton. Syst.*, vol. 70, pp. 215–226, Aug. 2015.
- [47] R. S. Inoue, M. H. Terra, and V. Grassi, Jr., "Robust state-space estimation for mobile robot localization," in *Proc. Latin Amer. Robot. Symp. Intell. Robot. Meeting*, Oct. 2008, pp. 85–90.
- [48] A. Boukerche, H. A. B. Foliveira, E. F. Nakamura, and A. A. F. Loureiro, "Vehicular ad hoc networks: A new challenge for localization-based systems," *Comput. Commun.*, vol. 31, no. 12, pp. 2838–2849, 2008.
- [49] J. González *et al.*, "Mobile robot localization based on ultra-wide-band ranging: A particle filter approach," *Robot. Auton. Syst.*, vol. 57, no. 5, pp. 496–507, 2009.
- [50] I. Abuhadrous, S. Ammoun, F. Nashashibi, F. Goulette, and C. Laugeau, "Digitizing and 3D modeling of urban environments and roads using vehicle-borne laser scanner system," in *Proc. IEEE/RSJ Int. Conf. Intell. Robots Syst. (IROS)*, vol. 1, Sep./Oct. 2004, pp. 76–81.
- [51] J. Clark and R. Fierro, "Mobile robotic sensors for perimeter detection and tracking," *ISA Trans.*, vol. 46, no. 1, pp. 3–13, 2007.
- [52] G. S. Rodríguez, "Obstacle detection based on laser range data and segmentation for an autonomous vehicle," M.S. thesis, Blaise Pascal Univ., Aubière, France, 2014.
- [53] L. Adouane, A. Benzerrouk, and P. Martinet, "Mobile robot navigation in cluttered environment using reactive elliptic trajectories," in *Proc. 18th IFAC World Congr.*, Aug. 2011, pp. 13801–13806.
- [54] J. Vilca, L. Adouane, and Y. Mezouar, "Reactive navigation of a mobile robot using elliptic trajectories and effective online obstacle detection," *Gyroscope Navigat.*, vol. 4, no. 1, pp. 14–25, 2013.
- [55] A. De Luca, G. Oriolo, and C. Samson, "Feedback control of a nonholonomic car-like robot," in *Robot Motion Planning and Control*, J.-P. Laumond, Ed. Berlin, Germany: Springer-Verlag, 1998, pp. 171–253.
- [56] J. Vilca, L. Adouane, Y. Mezouar, and P. Lébraly, "An overall control strategy based on target reaching for the navigation of an urban electric vehicle," in *Proc. IEEE/RSJ Int. Conf. Intell. Robots Syst. (IROS)*, Tokyo, Japan, Nov. 2013, pp. 728–734.
- [57] L. Adouane, "Architectures de contrôle comportementales et réactives pour la coopération d'un groupe de robots mobiles," Ph.D. dissertation, Univ. Franche-Comte, Besançon, France, Apr. 2005.
- [58] L. Adouane, "Orbital obstacle avoidance algorithm for reliable and online mobile robot navigation," in *Proc. 9th Conf. Auton. Robot Syst. Competitions*, Castelo Branco, Portugal, May 2009.
- [59] J. Vilca, L. Adouane, and Y. Mezouar, "Optimal multi-criteria waypoint selection for autonomous vehicle navigation in structured environment," *J. Intell. Robot. Syst.*, vol. 82, no. 2, pp. 301–324, May 2016.
- [60] S. Mastellone, D. M. Stipanović, C. R. Graunke, K. A. Intlekofer, and M. W. Spong, "Formation control and collision avoidance for multi-agent non-holonomic systems: Theory and experiments," *Int. J. Robot. Res.*, vol. 27, no. 1, pp. 107–126, 2008.
- [61] C. Ze-Su, Z. Jie, and C. Jian, "Formation control and obstacle avoidance for multiple robots subject to wheel-slip," *Int. J. Adv. Robot. Syst.*, vol. 9, no. 5, p. 188, 2012.
- [62] J. Vilca, L. Adouane, and Y. Mezouar, "Adaptive leader-follower formation in cluttered environment using dynamic target reconfiguration," in *Proc. Int. Symp. Distrib. Auton. Robot. Syst. (DARS)*, Daejeon, South Korea, Nov. 2014, pp. 727–734.
- [63] M. El Zaher, J.-M. Contet, F. Gechter, and A. Koukam, "Echelon platoon organisation: A distributed approach based on 2-spring virtual links," in *Proc. 15th Int. Conf. Artif. Intell., Methodol., Syst., Appl. (AIMSA)*, Berlin, Germany, 2012, pp. 246–255.
- [64] L. Consolini, F. Morbidi, D. Prattichizzo, and M. Tosques, "Leader-follower formation control of nonholonomic mobile robots with input constraints," *Automatica*, vol. 44, no. 5, pp. 1343–1349, 2008.
- [65] G. Klančar, D. Matko, and S. Blažič, "A control strategy for platoons of differential drive wheeled mobile robot," *Robot. Auton. Syst.*, vol. 59, no. 2, pp. 57–64, 2011.
- [66] D. G. Kendall, "A survey of the statistical theory of shape," *Statist. Sci.*, vol. 4, no. 2, pp. 87–99, 1989.
- [67] H. K. Khalil, *Nonlinear Systems*, 3rd ed. Upper Saddle River, NJ, USA: Prentice-Hall, 2002.
- [68] The Institut Pascal Data Sets. (Nov. 2017). [Online]. Available: <http://ipds.univ-bpclermont.fr> and <http://ipds.univ-bpclermont.fr>
- [69] S. Parkinson, P. Ward, K. Wilson, and J. Miller, "Cyber threats facing autonomous and connected vehicles: Future challenges," *IEEE Trans. Intell. Transp. Syst.*, vol. 18, no. 11, pp. 2898–2915, Nov. 2017.
- [70] Q. Li, L. Chen, M. Li, S.-L. Shaw, and A. Nuchter, "A sensor-fusion drivable-region and lane-detection system for autonomous vehicle navigation in challenging road scenarios," *IEEE Trans. Veh. Technol.*, vol. 63, no. 2, pp. 540–555, Feb. 2014.
- [71] M. S. Darms, P. E. Rybski, C. Baker, and C. Urmson, "Obstacle detection and tracking for the urban challenge," *IEEE Trans. Intell. Transp. Syst.*, vol. 10, no. 3, pp. 475–485, Sep. 2009.
- [72] Y. Cui and S. S. Ge, "Autonomous vehicle positioning with GPS in urban canyon environments," *IEEE Trans. Robot. Autom.*, vol. 19, no. 1, pp. 15–25, Feb. 2003.
- [73] R. W. Wolcott and R. M. Eustice, "Visual localization within LIDAR maps for automated urban driving," in *Proc. IEEE/RSJ Int. Conf. Intell. Robots Syst. (IROS)*, Sep. 2014, pp. 176–183.



**José Vilca** received the B.Eng. degree in electronic engineering from the National University of Engineering, Peru, in 2006, the M.Sc. degree in dynamic system from the University of São Paulo, Brazil, in 2011, and the Ph.D. degree in robotics from the Institut Pascal, UMR 6602, CNRS/Université Blaise Pascal, France, in 2015. He was with the Image, Perception Systems, Robotics Group, Institut Pascal. His research interests include cooperative systems, hybrid control systems, multi-robots coordination, robotics, and mobile-robot autonomous navigation and nonlinear control.



**Louis Adouane** received the Ph.D. degree in automatic control from the FEMTO-ST Laboratory, ENSMM, France, in 2005. During his Ph.D. studies, he deeply investigated the field of mobile multi-robot systems, especially those related to bottom-up and decentralized control architectures. In 2005, he joined the Ampère Laboratory, INSA Lyon, and he studied hybrid (continuous/discrete) control architectures applied to cooperative mobile robots arms. Since 2006, he has been an Associate Professor at the Institut Pascal, Polytech Clermont-Ferrand.

He had the opportunity to visit several institutions/laboratories, such as in 2014 at Cranfield and Kingston universities, U.K., and in 2018 at the Karlsruhe Institute of Technology, Germany. He is the author/co-author of more than 80 refereed international papers and two books. His main research interests include planning and control, hybrid (continuous/discrete) and hybrid (reactive/cognitive) multi-controller architectures, Lyapunov-based synthesis and stability, obstacle avoidance, cooperative multi-robot systems, navigation in formation, artificial intelligence (such as Markov decision process, multi-agent systems, or fuzzy logic), energy management (optimal control and neuro-fuzzy approaches), and multi-robot/agent simulation. He is currently a member of the Technical Committee of IFAC—Intelligent Autonomous Vehicles. In 2015, he obtained an HDR (habilitation to steer research in robotics) from Blaise Pascal University. He also serves as an Editorial Board Member of the *Journal of Intelligent and Robotic Systems*.



**Youcef Mezouar** received the Ph.D. degree in computer science from the Université de Rennes 1, Rennes, France, in 2001, and the Habilitation à Diriger les Recherches degree from Université Blaise Pascal, Clermont-Ferrand, France, in 2009. He is currently a Professor at the Institut Français de Mécanique Avancée and a member of the Institut Pascal, UMR 6602, CNRS/Université Blaise Pascal, France. He is a Co-Leader of the Image, Perception Systems, Robotics Group, Institut Pascal, and he also leads the Modeling, Autonomy and Control

in Complex Systems Team, Institut Pascal. His research interests include automatics, robotics, and computer vision, particularly visual servoing and mobile-robot navigation.